The spectrum of low- p_T J/ψ in heavy ion collisions in a fractal description

Huiqiang $\mathrm{Ding}^{1\dagger},\ \mathrm{Luan}\ \mathrm{Cheng}^{1,2^*\dagger},\ \mathrm{Tingting}\ \mathrm{Dai}^1,\ \mathrm{Enke}\ \mathrm{Wang}^2,\ \mathrm{Wei-Ning}\ \mathrm{Zhang}^1$

*Corresponding author(s). E-mail(s): luancheng@dlut.edu.cn;

†These authors contributed equally to this work.

Abstract

Transverse momentum spectrum of particles in hadron gas are affected by flow, quantum and strong interaction effects. Previously, most models are focused on only one of the three effects but ignore others. The unconsidered effects are taken into the fitted parameters. In this paper, we try to study the three effects together from a new fractal angle by physical calculation instead of data fitting. Near the critical temperature, the three effects together induce J/ψ and neighbouring meson to form a two-meson structure. We set up a two-particle fractal model (TPF model) to describe this structure. In our model, we propose that under the three effects, $J/\psi - \pi$ two-meson state, J/ψ and π two-quark states form a self-similarity structure. With the evolution, the two-meson structure disintegrate. We introduce an influencing factor q_{fqs} to describe the flow, quantum and strong interaction effects and an escort factor q_2 to describe the binding force between c and \bar{c} and the three effects. By solving the probability and entropy equations, we obtain the values of q_{fqs} and q_2 at different collision energies and centrality classes. By substituting the value of q_{fqs} into distribution function, we obtain the transverse momentum spectrum of low- $p_T J/\psi$ and find it in good agreement with experimental data. We also analyze the evolution of q_{fqs} with the temperature. It is found that q_{fqs} is larger than 1 and decreases with decreasing the temperature. This is because the three effects decrease the number of microstates, so that $q_{fqs} > 1$. q_{fqs} decreasing with the system evolution is consistent with the fact that with the system expansion, the influence of the three effects decreases. TPF model can be used to study other mesons and resonance states in the future.

Keywords: Transverse momentum spectrum, J/ψ distribution, Fractal theory

1 Introduction

Identified particle spectrum in transverse momenta are pillars in the discoveries of heavy ion collisions [1, 2]. This led to the study of transverse momentum distributions of identified particles sparking an intense activity in this field [3–6]. Among the identified particles, J/ψ is produced

at the early stage of collisions and interacts with the surroundings during the whole evolution of the system[7, 8]. So J/ψ carries significant information and the study of transverse momentum spectrum of J/ψ is significantly important[9, 10].

Charmonium dissociates in QGP[11] and can regenerate by a coalescence of c and \bar{c} quarks close

^{1*}School of Physics, Dalian University of Technology, Dalian, 116024, Liaoning, China.
²Institute of Quantum Matter, South China Normal University, Guangzhou, 510631, Guangdong, China.

to the hadronization transition[12]. Except production, other reactions which induce the change of particle number influence very little compared to the dissociation and regeneration process[13]. So the particle number of J/ψ is nearly constant after regeneration. We can study the particle number distribution after the regeneration process and compare it with the experimental data. After regeneration, J/ψ is influenced by the surrounding hadrons from three aspects: (i) J/ψ is influenced by the collective flow effect of the expanding hadron gas [14, 15]. (ii) J/ψ has a quantum correlation with the neighbouring hadron in a limited region[16]. (iii) J/ψ interacts with the neighbouring hadron[17, 18]. Statistical models are proposed to study the particle number distribution in recent years[19-25]. The typical and representative models are Tsallis blast-wave (TBW) model[19] and statistical hadronization model(SHM)[20, 21]. The TBW model concentrates on aspect (i)-the collective flow effect, but ignores aspects (ii) and (iii)[19]. The SHM model considers aspects (ii) and (iii)-the interactions and quantum correlation effects, but ignores aspect (i)[20, 21]. Although these models consider only one or two different effects and ignore others, their theoretical results can all be compared well with the experimental data. This is because the parameters in their models are obtained by data fitting. The unconsidered effects are taken into the fitted parameters [19–22]. So, it's meaningful and instructive to study the particle number distribution by physical calculation instead of by fitting.

In this paper, we will study the transverse momentum spectrum of J/ψ from a new angle and obtain the particle distribution by physical calculation instead of data fitting. We analyze J/ψ is influenced by the hadron gas as the following. Near the critical temperature, J/ψ is influenced by hadron gas through collective flow[14, 15], quantum and strong interaction effects [16–18]. With the system expansion and temperature decreasing, the influence decreases. We analyze the physical process and set up a two-particle fractal(TPF) model to study the thermal properties. Near the critical temperature, the collective flow, quantum and strong interaction induce a J/ψ - π two-hadron molecule state [26]. From the whole picture, the J/ψ - π molecule state shows a two-body structure. From the partial picture, the quarks inside

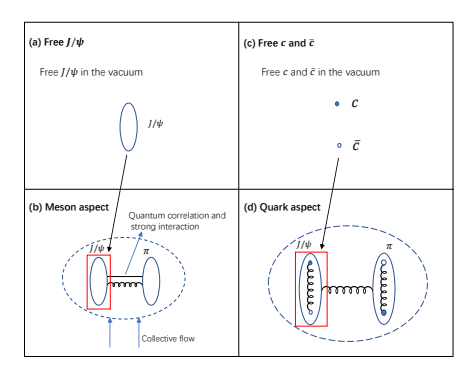


Fig. 1 The self-similarity structure of c and \bar{c} in the hadron gas near the critical temperature.

 J/ψ and π also show two-quark structure. In our model, we propose that J/ψ - π molecule state, J/ψ and π meson form a self-similarity structure [27] as shown in Fig. 1(d). With the system expansion, the two-meson molecule state and the selfsimilarity structure disintegrate. We will use the fractal theory to describe the self-similarity structure near the critical temperature, and introduce an influencing factor q_{fqs} to reflect the flow, quantum and strong interaction effects on J/ψ , an escort factor q_2 to denote the influence of binding interaction, flow, quantum and strong interaction effects on quarks. By solving the probability and entropy equations, we will obtain the values of q_{fqs} and q_2 through physical calculation instead of data fitting. By substituting the obtained q_{fgs} into the distribution of J/ψ , we will calculate the transverse momentum spectrum and compare it with the experimental data.

2 Charmonium in hadron gas

After regeneration, the particle number of low- p_T J/ψ is nearly constant[13]. So we can study the transverse momentum spectrum by analyzing the particle distribution of low- p_T J/ψ after regeneration. Near the critical temperature, the particle distribution is influenced from three points: (i) in the hadron gas, J/ψ co-moves with the neighbouring hadron(may well be pion)[14, 15]. (ii) J/ψ has quantum correlation with the neighbouring hadron[16]. In the space outside J/ψ with the diameter 2λ , J/ψ is easy to form quantum correlation with the neighbouring hadron. Where λ is the wavelength of J/ψ with $\lambda = h/\sqrt{2\pi mkT} = 0.681$ fm [28]. This space with diameter $2\lambda = 1.362$ fm can accommodate a pion

according to that the density of pion is $0.5/\text{fm}^3[16]$ and the distance of pion is 1.3 fm[16]. So that J/ψ and the nearest neighbouring pion has quantum correlation. (iii) J/ψ has strong interaction with the neighbouring pion[17, 18, 29]. From the Schrödinger equation, it is found that c quark has large probability to interact with other quarks if the distance is smaller than 0.8 fm[29]. So besides inside J/ψ c quark can interact with \bar{c} antiquark, outside J/ψ c quark can also interact with other quarks in other hadrons in the distance less than 0.8 fm. According to the pion density [16], J/ψ and its nearest neighbouring pion interacts and this must be taken into account. Overall, the collective flow, quantum correlation and strong interaction effects influence low- p_T J/ψ and the nearest neighbouring pion. Near the critical temperature, these two mesons form a twobody molecule-state system as shown in Fig. 1(b). From the quark aspect, inside the meson, the quark and anti-quark form a two-quark bounded system. So in our model, we propose that near the critical temperature, the J/ψ - π two-meson system from the whole picture, J/ψ and π twoquark system from the partial picture satisfies self-similarity[27]. Fractal owns the character of self-similarity and self-affinity, and can reflect the similarity in the field of statistics[27, 30]. So we will use the fractal theory to study the J/ψ - π self-similarity structure. With the system expansion, the distance between mesons increases, most molecule states disintegrate. So the self-similarity structure vanish.

Near the critical temperature, we firstly study the charmonium in vacuum from quarkonium aspect as shown in Fig. 1(a).

In the center of mass frame, if we firstly assume the charmonium in a vacuum and free, the probability of the charmonium at J/ψ state is

$$P1_{1} = \frac{\langle \psi_{1} | e^{-\beta \hat{H}} | \psi_{1} \rangle}{\sum_{i} \langle \psi_{i} | e^{-\beta \hat{H}} | \psi_{i} \rangle}, \tag{1}$$

where ψ_i is the wave function, the state ψ_1 corresponds to J/ψ . \hat{H} is the Hamiltonian of the charmonium in the vacuum, $\hat{H} = \frac{\hat{P}_{Q1}^2}{2m_Q} + \frac{\hat{P}_{Q2}^2}{2m_Q} + \hat{V}_{\text{vac}}(r)$, r is the distance between c and \bar{c} , $m_Q = 1.275\,\text{GeV}$. The partition function $\sum_i \langle \psi_i | e^{-\beta \hat{H}} | \psi_i \rangle$ is the sum of probabilities over

all microstates,

$$\sum_{i} \langle \psi_{i} | e^{-\beta \hat{H}} | \psi_{i} \rangle = e^{-\beta E_{0}} + e^{-\beta E_{1}} + \dots + e^{-\beta E_{7}} + V \int_{|\vec{p}_{Q1}| \ge p_{\min}}^{\infty} \int_{|\vec{p}_{Q2}| \ge p_{\min}}^{\infty} \int_{r_{\min}}^{r_{\max}} e^{-\beta (\frac{p_{Q1}^{2}}{2m_{Q}} + \frac{p_{Q2}^{2}}{2m_{Q}} + V_{\text{vac}}(r))} 4\pi r^{2} \frac{d^{3} \vec{p}_{Q1} d^{3} \vec{p}_{Q2} dr}{(2\pi)^{6}}.$$
(2)

For the lower discrete energy levels, we sum up the eight discrete ones $\eta_c(1S)$, $J/\psi(1S)$, $h_c(1P)$, $\chi_{c0}(1P), \ \chi_{c1}(1P), \ \chi_{c2}(1P), \ \eta_{c}(2S) \ \text{and} \ \psi(2S)$ which are measured at experiment[31]. $E_0, E_1, ...,$ E_7 are the energies of the eight discrete states. For the energy levels higher than $\psi(2S)$, the energies are nearly continuous[31], for convenience of calculation, we integrate the higher energy levels. p_{\min} is the minimum momentum of the higher levels part. Because the difference of the momentum at adjoint energy levels is little[31], we take the momentum of $\psi(2S)$ state, which is the highest energy level of the eight discrete states, as p_{\min} here. V is the volume of the charmonium's motion relative to the surrounding particles with a radius r_0 . Here the value of r_0 is not fixed but changes with collision energy $\sqrt{s_{\mathrm{NN}}}$ and centrality. We have $r_0 = (v\tau + d_{J/\psi} + d_{\pi})/2$, where v is the mean velocity of the surrounding particles relative to J/ψ , which can be obtained from average p_T of them. τ is the lifetime of J/ψ in the medium, $\tau = 1/\Gamma \approx 1/0.03 \,\text{GeV}^{-1}[32], d_{J/\psi}$ and d_{π} are the diameters of J/ψ and pion with $d_{J/\psi} + d_{\pi} \approx 2 \,\mathrm{fm}[29].$

Table 1 The values of r_0 at different collision energies and centrality classes.

Au-Au $\sqrt{s_{ m NN}}$	$r_0(\mathrm{fm})$			
	0-20%	20-40%	0-60%	
$39\mathrm{GeV}$	3.74	3.66	3.67	
$62.4\mathrm{GeV}$	3.83	3.76	3.76	
$200\mathrm{GeV}$	3.91	3.84	3.85	

The values of r_0 which are calculated at different collision energies $\sqrt{s_{\mathrm{NN}}}$ and centrality classes are shown in Table. 1. The average p_T are obtained from experimental data[33, 34] and AMPT data[35]. For $\sqrt{s_{\mathrm{NN}}} = 62.4\,\mathrm{GeV}$, v = 0.831, 0.809, 0.811 for 0-20%, 20-40%, 0-60%

centrality respectively. For $\sqrt{s_{\mathrm{NN}}}=200\,\mathrm{GeV},$ v=0.884,0.865,0.867 for 0-20%, 20-40%, 0-60% centrality. For $\sqrt{s_{\mathrm{NN}}}=39\,\mathrm{GeV},$ v=0.831,0.809,0.811 for 0-20%, 20-40%, 0-60% centrality. It shows that at higher collision energies or more central collisions, r_0 is larger. In Eq.(2), r_{min} and r_{max} are the lower and upper limits of the distance between c and \bar{c} . We take the value of radius of the motion volume r_0 as r_{max} , and the minimal spacing 0.05 fm in Ref.[36] as r_{min} .

In the Hamiltonian of the charmonium in Eq.(1) and Eq.(2), $V_{\text{vac}}(r)$ is the heavy quark potential in a vacuum as [37, 38]

$$V_{\rm vac}(r) = -\frac{\alpha_s}{r} + \sigma r - \frac{0.8\sigma}{m_Q^2 r},\tag{3}$$

where α_s is the strong coupling constant with α_s =0.385[38], the string tension σ =0.223 GeV²[38].

The above probability of J/ψ is considered in a vacuum. However, J/ψ is not placed in a vacuum and free, but lies in and interacts with the surrounding hadrons[14–18]. Due to the flow, quantum and strong interaction effects from the surroundings, J/ψ and the neighbouring hadron form a self-similar two-body system as shown in Fig. 1(b). So the probability of J/ψ in the hadron gas is the escort probability [39], which is the power of the probability in the vacuum $P1_1[40, 41]$. We introduce an influencing factor q_{fqs} to represent the flow, quantum and strong interaction effects, so we have

$$P1_{q} = \frac{P1_{1}^{q_{fqs}}}{\sum_{i} P1_{i}^{q_{fqs}}} = \frac{\langle \psi_{1} | e^{-\beta q_{fqs} \hat{H}} | \psi_{1} \rangle}{\sum_{i} \langle \psi_{i} | e^{-\beta q_{fqs} \hat{H}} | \psi_{i} \rangle}. \quad (4)$$

When q_{fqs} equals 1, Eq.(4) is the same as Eq.(1), this implies there is no influence. The more q_{fqs} deviates from 1, the stronger J/ψ is influenced.

The interactions we considered here are all strong interactions. In weak coupling area, the interaction potential is proportional to $r^{-\alpha}$ with $\alpha=1[38]$. In the strong coupling area, the potential is proportional to $r^{-\alpha}$ with $\alpha=-1[38]$. As the reference [42] defines, for the interaction potential $V(r)\approx r^{-\alpha}$, if $\alpha/d\leq 1(d$ is the dimension of the system, here we consider d=3), the interaction is a long-range interaction. So according to the form of the strong interaction here, no matter it is strongly coupled or weakly coupled, is long-range

interaction. Tsallis entropy is proved to describe long-range interaction system very well[47]. Here, we will use the Tsallis entropy to describe the charmonium system,

$$S1_{q} = \frac{1 - \sum_{i} P1_{i}^{q_{fqs}}}{q_{fqs} - 1}$$

$$= \left(1 - \frac{\sum_{i} \langle \psi_{i} | e^{-\beta q_{fqs} \hat{H}} | \psi_{i} \rangle}{(\sum_{i} \langle \psi_{i} | e^{-\beta \hat{H}} | \psi_{i} \rangle)^{q_{fqs}}}\right) / (q_{fqs} - 1).$$
(5)

The above analysis is carried out from charmonium aspect. Secondly, we will study from quark aspect as shown in Fig. 1(c) and Fig. 1(d).

If the quark and anti-quark are free, in the center of mass frame, the probability of the two-quark system with the energy the same as the kinetic energy of J/ψ is

$$P2_{1} = \frac{\langle \phi_{1} | e^{-\beta \hat{H}_{0}} | \phi_{1} \rangle}{\sum_{i} \langle \phi_{i} | e^{-\beta \hat{H}_{0}} | \phi_{i} \rangle}, \tag{6}$$

where ϕ_i is the wave function of the two-quark system, ϕ_1 corresponds to state with kinetic energy equals to J/ψ , $\hat{H_0} = \frac{\hat{P}_{Q1}^2}{2m_Q} + \frac{\hat{P}_{Q2}^2}{2m_Q}$, which is the Hamiltonian of the two-quark system. The partition function $\sum_i \left<\phi_i\right| e^{-\beta \hat{H_0}} \left|\phi_i\right>$ is the sum of probabilities of the two-quark system of all the microstates. Similarly to the previous case, we integrate the higher energy levels and sum up the eight discrete lower energy levels. The partition function can be written as

$$\sum_{i} \langle \phi_{i} | e^{-\beta \hat{H_{0}}} | \phi_{i} \rangle = e^{-\beta E_{k0}} + e^{-\beta E_{k1}} + \dots + e^{-\beta E_{k7}} + V^{2} \int_{|\vec{p}_{Q1}| \ge p'_{\min}}^{\infty} \int_{|\vec{p}_{Q2}| \ge p'_{\min}}^{\infty} e^{-\beta (\frac{\vec{p}_{Q1}^{2}}{2m_{Q}} + \frac{\vec{p}_{Q2}^{2}}{2m_{Q}})} \frac{d^{3} \vec{p}_{Q1} d^{3} \vec{p}_{Q2}}{(2\pi)^{6}}$$
(7)

We take the momentum of $\psi(2S)$ as the minimum momentum of the higher levels. Here E_{k0} , $E_{k1}, ..., E_{k7}$ are the kinetic energies of c and \bar{c} at the eight discrete states. They are obtained from the non-relativistic Schrödinger equation,

$$\hat{H}\psi_i(r) = E_i\psi_i(r),\tag{8}$$

where
$$\hat{H} = \hat{H}_{\text{kinetic}} + \hat{V}_{\text{vac}}(r) = \frac{\hat{P}_{Q1}^2}{2m_Q} + \frac{\hat{P}_{Q2}^2}{2m_Q} + \hat{V}_{\text{vac}}(r)$$
.

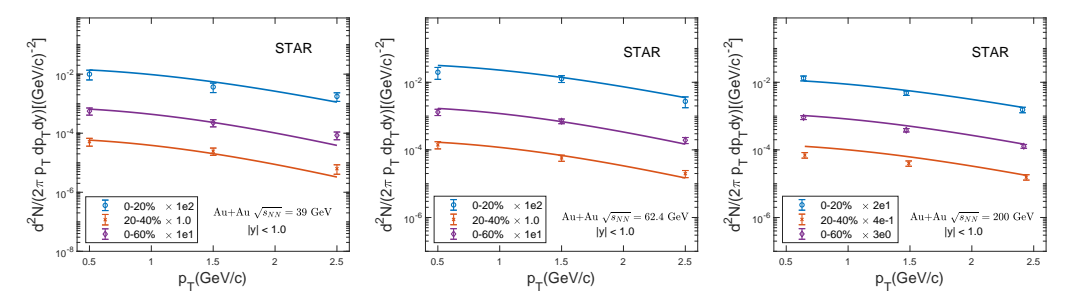


Fig. 2 Transverse momentum spectra of J/ψ in Au-Au collisions at $\sqrt{s_{\rm NN}}=39\,{\rm GeV}, 62.4\,{\rm GeV}, 200\,{\rm GeV}$ for different centrality classes, in mid-rapidity region |y|<1.0. The experimental data are taken from STAR[45, 46].

The above calculation is carried out by assuming the quark and anti-quark to be free. However, the quark and anti-quark are not free, they are bounded together and influenced by the flow, quantum and strong interaction effects[14–18]. All these lead to the quark and anti-quark pair forming quarkonium in the hadron gas, and the quarkonium and the neighbouring hadron form two-meson structure as shown in Fig. 1(d). We introduce an escort factor q_2 to denote the influence of the binding interaction between c and \bar{c} , and the flow, quantum, strong interaction effects. Using the fractal theory, the escort probability of the $c\bar{c}$ quark and anti-quark pair at J/ψ state is[39–41]

$$P2_{q_2} = \frac{P2_1^{q_2}}{\sum_i P2_i^{q_2}} = \frac{\langle \phi_1 | e^{-\beta q_2 \hat{H_0}} | \phi_1 \rangle}{\sum_i \langle \phi_i | e^{-\beta q_2 \hat{H_0}} | \phi_i \rangle}, \quad (9)$$

when q_2 equals 1, Eq.(9) turns to be same as Eq.(6). This implies no effect. The more q_2 deviates from 1, the larger the system is influenced.

For the interactions are long-ranged, similar to Eq.(5), the Tsallis entropy of the quark and anti-quark pair can be written as [47]

$$S2_{q_2} = \frac{1 - \sum_{i} P2_i^{q_2}}{q_2 - 1}$$

$$= (1 - \frac{\sum_{i} \langle \phi_i | e^{-\beta q_2 \hat{H_0}} | \phi_i \rangle}{(\sum_{i} \langle \phi_i | e^{-\beta \hat{H_0}} | \phi_i \rangle)^{q_2}}) / (q_2 - 1).$$
(10)

Overall, we have analyzed the probability and entropy of the c, \bar{c} quark and anti-quark pair from quarkonium and quark aspects. Although we consider the system from different aspects, the properties of the system should be the same, so

we have

$$P1_q = P2_{q_2};$$
 (11)

$$S1_q = S2_{q_2}.$$
 (12)

By solving the conservation equations of probability and entropy Eq.(11) and Eq.(12), we can obtain the values of two variables q_{fqs} and q_2 . Shown in Table.2 is the values of influencing factors q_{fqs} and q_2 in Au-Au collisions at $\sqrt{s_{\mathrm{NN}}}{=}39$, 62.4, 200 GeV in mid-rapidity region $|y| \leq 1.0$ for different centrality classes. All the values here are obtained totally through physical calculation without any data fitting. We can find that the value of q_2 is larger than q_{fqs} in the same collision. This is because compared to q_{fqs} , q_2 considers one more binding interaction between c and \bar{c} . So the value of q_2 deviates more from 1.

Table 2 The influencing factors q_{fqs} and q_2 in Au-Au collisions at $\sqrt{s_{\mathrm{NN}}}=39\,\mathrm{GeV},\,62.4\,\mathrm{GeV},\,200\,\mathrm{GeV}$ in mid-rapidity region |y|<1.0 for different centrality classes.

Au-Au $\sqrt{s_{ m NN}}$		Centrality		
Tra Tra Volvin		0-20%	20-40%	0-60%
$39\mathrm{GeV}$	q_{fqs} q_2	1.0343 1.5186	$1.0246 \\ 1.5208$	1.0258 1.5205
$62.4\mathrm{GeV}$	q_{fqs} q_2	$1.0450 \\ 1.5162$	$1.0367 \\ 1.5181$	1.0367 1.5181
$200\mathrm{GeV}$	q_{fqs} q_2	1.0542 1.5139	1.0461 1.5158	1.0473 1.5156

By substituting the obtained q_{fqs} into particle number distribution, the transverse momentum spectrum of low- p_T J/ψ can be obtained. The distribution of the particle number can be written as[6]

$$\frac{d^2N}{2\pi p_T dp_T dy} = V_{\text{lab}} \frac{m_T \cosh y}{(2\pi)^3} f_i, \qquad (13)$$

where f_i is the distribution function, $f_i = [(1 + (q_{fqs}-1)\beta m_T \cosh y)^{q_{fqs}/(q_{fqs}-1)}-1]^{-1}[43], m_T$ is the transverse mass of J/ψ with $m_T = \sqrt{m^2 + p_T^2}$, m is the mass of J/ψ with m = 3.096 GeV, p_T is the transverse momentum in the lab frame. V_{lab} is J/ψ 's motion volume in the lab frame with $V_{\text{lab}} = \gamma V$, γ is the Lorentz factor.

Shown in Fig. 2 is the transverse momentum spectrum of low- p_T J/ψ for Au-Au collisions at $\sqrt{s_{\mathrm{NN}}} = 39$, 62.4, 200 GeV and 0-20%, 20-40%, 0-60% centrality classes. We compare our theoretical results with the experimental data[45, 46] at low- p_T region. Our theoretical results show a good agreement with the experimental data.

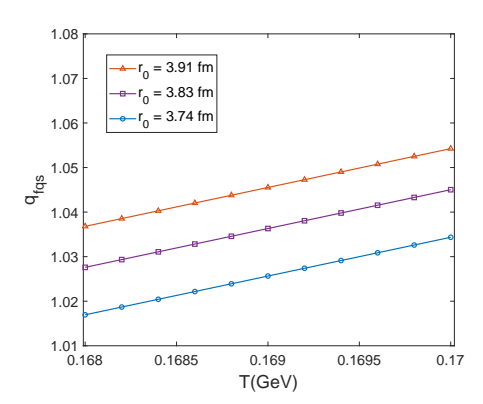


Fig. 3 The influencing factor q_{fqs} at different fixed temperature with $r_0=3.74,3.83,3.91\,\mathrm{fm}.$

We also study the evolution of q_{fqs} with the temperature. Shown in Fig. 3 is the influencing factor q_{fqs} at different fixed temperature with $r_0=3.74,\ 3.83,\ 3.91$ fm, which is the radius of motion volume of the charmonium relative to surrounding particles at $\sqrt{s_{\mathrm{NN}}}=39,\ 62.4\ 200$ GeV for 0-20% centrality. It is found that q_{fqs} is larger than 1. This comes from that for Tsallis entropy, $S_{\mathrm{q}}< S_{\mathrm{B-G}}$ if q>1[44]. Here the three effects induce the two-meson structure and decrease the number of microstates. So the entropy is decreased and the value of q_{fqs} is larger than 1. At fixed r_0 , the value of q_{fqs} decreases with decreasing the temperature. This is consistent with the fact that

 J/ψ is typically influenced near critical temperature. With the system expansion and temperature decreasing, the influence decreases. So q_{fqs} decreases to approaching 1. It is also found that at fixed temperature, the influencing factor q_{fqs} increases with increasing r_0 . This is because in a larger motion volume, the probability of the charmonium being influenced by the surroundings is larger, so that the influencing factor q_{fqs} is larger.

3 Conclusion

We study the low- p_T transverse momentum spectrum of J/ψ by physical calculation instead of by data fitting. We analyze the particle number distribution of J/ψ after regeneration because after that the number of J/ψ is nearly constant. After regeneration J/ψ is influenced by flow, quantum and strong interaction effects. Under these effects, near the critical temperature, J/ψ and the nearest neighbouring meson may well form a twomeson structure. With the evolution of the system, the two-meson structure will disintegrate. We set up a two-particle fractal model(TPF model) to describe the two-meson structure. From the whole picture, J/ψ and π form a two-meson structure; from the partial picture, J/ψ and π show a twoquark structure. In our model, we propose that under the three effects, J/ψ - π molecule state, J/ψ and π form a self-similarity structure. We introduce an influencing factor q_{fqs} to describe the flow, quantum and strong interaction effects and an escort factor q_2 to describe the binding and the three effects. By solving the probability and entropy equations, we obtain the values of q_{fas} and q_2 at different collision energies and centrality classes. By substituting the value of q_{fqs} into distribution function, we obtain the transverse momentum spectrum of low- p_T J/ψ . We compare our calculation with the experimental data and find a good agreement. We also analyze the evolution of q_{fqs} with the temperature. It is found that q_{fas} is larger than 1. This is because the flow, quantum and strong interaction effects induce the two-meson structure and decrease the number of microstates. We also find that q_{fgs} decreases with decreasing the temperature. This is consistent with the fact that J/ψ is typically influenced near critical temperature, with the system expansion and temperature decreasing, the influence decreases. Our TPF model can be used to

study other mesons and resonance states in the future.

Acknowledgments. This work was supported by the National Natural Science Foundation of China under Grant No. 12175031, Guangdong Provincial Key Laboratory of Nuclear Science with No.2019B121203010.

References

- K. S. Lee, U. Heinz, E. Schnedermann, Z. Phys. C: Part. Fields 48, 525 (1990) https://doi.org/10.1007/BF01572035
- [2] L. Van Hove, Phys. Lett. B 118, 138 (1982) https://doi.org/10.1016/0370-2693(82)90617-7
- [3] B. I. Abelev, et al., Phys. Rev. C 79, 034909
 (2009) https://doi.org/10.1103/PhysRevC.79. 034909
- [4] P. Bożk, I. Wyskiel-Piekarska, Phys. Rev.
 C 85, 064915 (2012) https://doi.org/10.1103/ PhysRevC.85.064915
- [5] X. N. Wang, Phys. Rev. C 61, 064910 (2000) https://doi.org/10.1103/PhysRevC.61.064910
- [6] J. Cleymans, D. Worku, Eur. Phys. J. A 48, 160 (2012) https://doi.org/10.1140/epja/ i2012-12160-0
- [7] A. Andronic, et al., Eur. Phys. J. C 76, 107 (2016) https://doi.org/10.1140/epjc/ s10052-015-3819-5
- [8] N. Brambilla, et al., Eur. Phys. J. C 71, 1534 (2011). https://doi.org/10.1140/epjc/ s10052-010-1534-9
- [9] R. Rapp, D. Blaschke, P. Crochet, Prog. Part. Nucl. Phys. 65, 209 (2010) https://doi.org/10. 1016/j.ppnp.2010.07.002
- [10] A. Rothkopf, Phys. Rep. 858, 1 (2020) https: //doi.org/10.1016/j.physrep.2020.02.006
- [11] T. Matsui, H. Satz, Phys. Lett. B 178, 416
 (1986) https://doi.org/10.1016/0370-2693(86)
 91404-8

- [12] R. L. Thews, M. Schroedter, J. Rafelski, Phys. Rev. C 63, 054905 (2001) https://doi. org/10.1103/PhysRevC.63.054905
- [13] J. Zhao, K. Zhou, S. Chen, P. Zhuang, Prog. Part. Nucl. Phys. 114, 103801 (2020) https://doi.org/10.1016/j.ppnp.2020.103801
- [14] N. Herrmann, J. P. Wessels, T. Wienold, Annu. Rev. Nucl. Part. Sci. 49, 581 (1999) https://doi.org/10.1146/annurev.nucl.49.1.581
- [15] E. Schnedermann, J. Sollfrank, U. Heinz, Phys. Rev. C 48, 2462 (1993) https://doi.org/ 10.1103/PhysRevC.48.2462
- [16] C. Y. Wong, Phys. Rev. C 65, 034902 (2002) https://doi.org/10.1103/PhysRevC.65.034902
- [17] Z. Lin, C. M. Ko, Phys. Rev. C 62, 034903
 (2000) https://doi.org/10.1103/PhysRevC.62.
 034903
- [18] A. Bourque, C. Gale, K. L. Haglin, Phys. Rev.
 C 70, 055203 (2004) https://doi.org/10.1103/ PhysRevC.70.055203
- [19] Z. Tang, Y. Xu, L. Ruan, G. van Buren,
 F. Wang, Z. Xu, Phys. Rev. C 79, 051901(R)
 (2009) https://doi.org/10.1103/PhysRevC.79.
 051901
- [20] J. Cleymans, H. Satz, Z. Phys. C: Part. Fields 57, 135 (1993) https://doi.org/10.1007/ BF01555746
- [21] A. Andronic, P. Braun-Munzinger, K. Redlich, J. Stachel, Phys. Lett. B 571, 36 (2003) https://doi.org/10.1016/j.physletb.2003.07.066
- [22] A. Andronic, P. Braun-Munzinger, M. K. Köhler, K. Redlich, J. Stachel, Phys. Lett. B 797, 134836 (2019) https://doi.org/10.1016/j. physletb.2019.134836
- [23] L. N. Gao, F. H. Liu, B. C. Li, Adv. High Energy Phys. 2019, 6739315 (2019) https:// doi.org/10.1155/2019/6739315
- [24] Y. H. Chen, Y. G. Ma, G. L. Ma, J. H. Chen, J. Phys. G: Nucl. Part. Phys. 47, 045111 (2020) https://doi.org/10.1088/1361-6471/ab67e6

- [25] X. H. Zhang, F. H. Liu, K. K. Olimov, Int. J. Mod. Phys. E 30, 2150051 (2021) https://doi. org/10.1142/S0218301321500518
- [26] R. Aaij, et al., Phys. Rev. L 112, 222002 (2014) https://doi.org/10.1103/PhysRevLett. 112.222002
- [27] B. Mandelbrot, Science 156, 636 (1967) https://doi.org/10.1126/science.156.3775.636
- [28] R. K. Pathria, Paul D. Beale, Statistical mechanics (Elsevier, London, 2022), pp. 127-128 https://doi.org/10.1016/b978-0-08-102692-2.00014-4
- [29] H. W. Crater, J. H. Yoon, C. Y. Wong, Phys. Rev. D 79, 034011 (2009) https://doi.org/10. 1103/PhysRevD.79.034011
- [30] B. B. Mandelbrot, The fractal geometry of nature, vol. 1 (WH freeman New York, 1982), pp. 25–74
- [31] C. Patrignani, et al., Chin. Phys. C 40, 100001 (2016) https://doi.org/10.1088/ 1674-1137/40/10/100001
- [32] P. K. Srivastava, O.S.K. Chaturvedi, L. Thakur, Eur. Phys. J. C 78, 440 (2018) https://doi.org/10.1140/epjc/s10052-018-5912-z
- [33] L. Adamczyk, et al., Phys. Rev. C 96, 044904
 (2017) https://doi.org/10.1103/PhysRevC.96. 044904
- [34] S. Acharya, et al., Phys. Lett. B 805, 135434 (2020) https://doi.org/10.1016/j.physletb. 2020.135434
- [35] Z. W. Lin, C. M. Ko, B. A. Li, B. Zhang,
 S. Pal, Phys. Rev. C 72, 064901 (2005) https://doi.org/10.1103/PhysRevC.72.064901
- [36] M. Cè, T. Harris, H. B. Meyer, A. Toniato, C. Török, J. High Energy Phys. 2021, 215 (2021) https://doi.org/10.1007/JHEP12(2021)215
- [37] F. Karsch, M. T. Mehr, H. Satz, Z. Phys. C: Part. Fields 37, 617 (1988) https://doi.org/10. 1007/BF01549722

- [38] A. Dumitru, Y. Guo, Á. Mócsy, M. Strickland, Phys. Rev. D 79, 054019 (2009) https://doi.org/10.1103/PhysRevD.79.054019
- [39] C. Beck, F. Schögl, Thermodynamics of chaotic systems (Cambridge University Press, Cambridge, 1993), pp. 88-127 https://doi.org/ 10.1017/cbo9780511524585
- [40] T. Tél, Z. Naturforsch. A: Phys. Sci. 43a, 1154 (1988) https://doi.org/10.1515/ zna-1988-1221
- [41] M. Schroeder, Fractals, Chaos, Power Laws: Minutes from an Infinite Paradise. (W H Freeman and Company, New York, 1991), pp. 103-121
- [42] S. Abe, Y. Okamoto, Nonextensive statistical mechanics and its applications, vol. 560(Springer, Berlin, 2001), pp. 5-6 https://doi.org/10.1007/3-540-40919-x
- [43] C. Beck, Physica A **286**, 164 (2000) https://doi.org/10.1016/s0378-4371(00)00354-x
- [44] C. Tsallis, Introduction to nonextensive statistical mechanics: approaching a complex world, vol. 1 (Springer, Berlin, 2009), pp. 41-42 https://doi.org/10.1007/978-0-387-85359-8
- [45] L. Adamczyk, et al., Phys. Rev. C 90, 024906
 (2014) https://doi.org/10.1103/PhysRevC.90.
 024906
- [46] L. Adamczyk, et al., Phys. Lett. B 771, 13 (2017) https://doi.org/10.1016/j.physletb. 2017.04.078
- [47] C. Tsallis, J. Stat. Phys. 52, 479 (1988) https://doi.org/10.1007/BF01016429